韓國海岸海洋工學發表論文集 (2003)
第14券, pp. 164-169

Computation of Super High-Resolution Global Ocean Model using Earth Simulator

Dong-Hoon Kim[1], Norikazu Nakashiki[1], Yoshikatsu Yoshida[1], Takaki Tsubono[1], Frank O. Bryan[2], Richard D. Smith[3], Mathew E. Maltrud[3], Matthew W. Hecht[3], and Julie L. McClean[4]

1. INTRODUCTION

The need for higher grid resolution in climate models is often discussed (e.g. McAvaney et al., 2001) because a number of important oceanic processes are not resolved by the current generation of coupled models, e.g., boundary currents, mesoscale eddy fluxes, sill through flows.

McClean et al., (1997) and Bryan and Smith (1998) have compared simulated mesoscale variability in simulations at several eddy-resolving resolutions to TOPEX/Poseidon and similar data.

Recent numerical studies suggest that a grid spacing on the order of 0.1° is a threshold for a good representation of the western boundary currents and of the mesoscale eddy kinetic energy. The usefulness of such high-resolution simulations are evaluated here focusing on the enhanced regional features of surface circulations manifested in our eddy-resolving global ocean simulation carried out on the Earth Simulator. We compared the results of eddy-resolving simulations at 0.1°×0.1° resolution to that of eddy-permitting simulation at 1°×1° resolution. This paper has concentrated on a description of the time-mean circulation; thus our results do not assess possible sensitivity of simulated time variability to horizontal resolution.

2. MODEL CONFIGURATION

The simulations discussed here were all performed with the Parallel Ocean Program (POP) version 1 which is an ocean component of the Community Climate System Model (CCSM2). This model is based on the Bryan-Cox-Semtner class of models (Semtner, 1986) and is described in more detail by Smith and Gent Eds. (2002).

All simulations use a global domain, realistic, and unsmoothed topography. All cases are forced with monthly averaged climatological heat, fresh water and wind stress forcing derived from NCEP climatology data. Heat and salt fluxes are obtained by linear interpolation in time between climatological data. No restoring of SSTs to prescribed values is used and no acceleration techniques are used.

Four experiments, one with a horizontal mesh of 1°×1° and three with 0.1°×0.1° mesh, have been carried out that differ only in their horizontal resolution and horizontal mixing parameterization. Distinguishing features of our four simulations are listed in Table 1. All four simulations use the same 40 levels in the vertical. All simulations use KPP vertical mixing scheme.

Our baseline 0.1°×0.1° simulation (which we designate as ES_01A) uses Biharmonic horizontal viscosity and diffusivity. In the ES_01C simulation we used a viscosity and diffusion coefficients of 1/3 times less than those in ES_01A simulation.

By comparing the X1.02 results to the ES_01A results

[1] Central Research Institute of Electric Power Industry (CRIEPI), 1646 Abiko, Abiko-shi, Chiba-ken 270-1194, JAPAN
[2] National Center for Atmospheric Research (NCAR), Boulder CO, U.S.A.
[3] Los Alamos National Laboratory (LANL), Los Alamos NM, U.S.A.
[4] Naval Postgraduate School, Monterey CA, U.S.A.

Table 1. Distinguishing features of the simulations described here

Simulation	Horizontal Resolution	Pole	Horiz. Mixing for momentum (cm^2/s)	Horiz. Mixing for tracer (cm^2/s)	Vertical Mixing
X1.02	1°×1°	Greenland	Anisotropic viscosity	GM	KPP
ES_01A	0.1°×0.1°	Hudson	-2.7x10^18	-9.0x10^17	KPP
ES_01C	0.1°×0.1°	Hudson	1/3 times of ES_01A	1/3 times of ES_01A	KPP
ES_01D	0.1°×0.1°	Hudson	same as ES_01A	GM	KPP

Note: We do not describe ES_01B case, 1/2 times less than those in ES_01A, in this paper.

we can identify effects of changing the horizontal mesh; by comparing the ES_01A results to ES_01C and ES_01D results we can identify effects of changing horizontal mixing coefficients and scheme.

X1.02 simulation was run for 473 model years and all ES_01s simulations were run 15 model years. The all results showed here were averaged for last 5 model years and we first regridded the 0.1°×0.1° results to the 1°×1° mesh to compare the results for global.

3. RESULTS

Although the model covers global, we focus only some interesting region. Since the 0.1°×0.1° simulations can resolve ocean eddies, our results address the possible importance of resolving eddies. Detailed analyses of other regions will be reported elsewhere.

Fig. 1 shows the annual mean sea surface temperature for global. All model cases are similar to observation data and reproduce the general features of the global circulation of the ocean satisfactorily regardless of the difference in the horizontal resolution. The slightly underestimation of SST in the equatorial ocean is observed in all model cases. This is very common in most OGCMs and is due to the too strong South Equatorial Current and upwelling. This confirms that there is no relationship between the cold tongue problem and horizontal resolution.

Fig. 2 shows that there are significant differences between the 1°×1° and 0.1°×0.1° simulations, most notably in the western boundary currents and the Antarctic Ocean. In the 0.1°×0.1° resolution cases the intensity of western boundary currents are somewhat stronger than those of the 1°×1° resolution case. The subpolar gyre is stronger in most areas, indicating that eddy activity and flow topography interaction must have changed with resolution.

The simulated Kurshio Current, one of the most dramatic western boundary currents in the world oceans, is too broad and weak beyond the separation point in 1°×1° resolution (Fig. 3.). These shortcomings were remedied by 0.1°×0.1° resolution cases.

The large-scale features of the model solutions are very similar at the horizontal mixing scheme cases and more sensitive to a large difference in resolution than to the difference in horizontal viscosity and diffusivity. This suggests that increases in horizontal resolution which can resolve eddies will be more effective than other approaches inside the eddy-resolving regime.

The intrusion of the Tsushima Current into the East/Japan Sea and the East Korean Warm Current along the eastern coast of Korea are also resolved in the 0.1°×0.1° resolution cases. But there is a unrealistic anticyclonic cell near the separation point of East Korean Warm Current in ES_01A and ES_01C cases.

Aside from the crude representation of the coastlines in the one degree (approximately 100 km) resolution case, the major current systems can be identified. The Kuroshio Current appears as a broad band of flow along the coast. Clear deficiencies are the width and meandering of the Kuroshio Current, and the lack of the Ryukyu Current at 450 meter depth (Fig. 4).

In contrast, 0.1°×0.1° high resolution case has greatly improved flow fields. The Kuroshio Current is more energetic, the Ryukyu Current at 450 meter depth appears realistically. Both the more accurate coastline/bottom topography and the existence of an eddy field contribute to this improvement.

The 0.1°×0.1° resolution case show meandering at the south of Japan with a warm anticyclonic gyre associated with surface elevation. This gyre structure is also seen in the surface dynamic height field using the TOPEX/POSEIDON altimetry data.

Cross sections of zonal velocity, temperature, and salinity illustrate the internal structure below the sea surface.

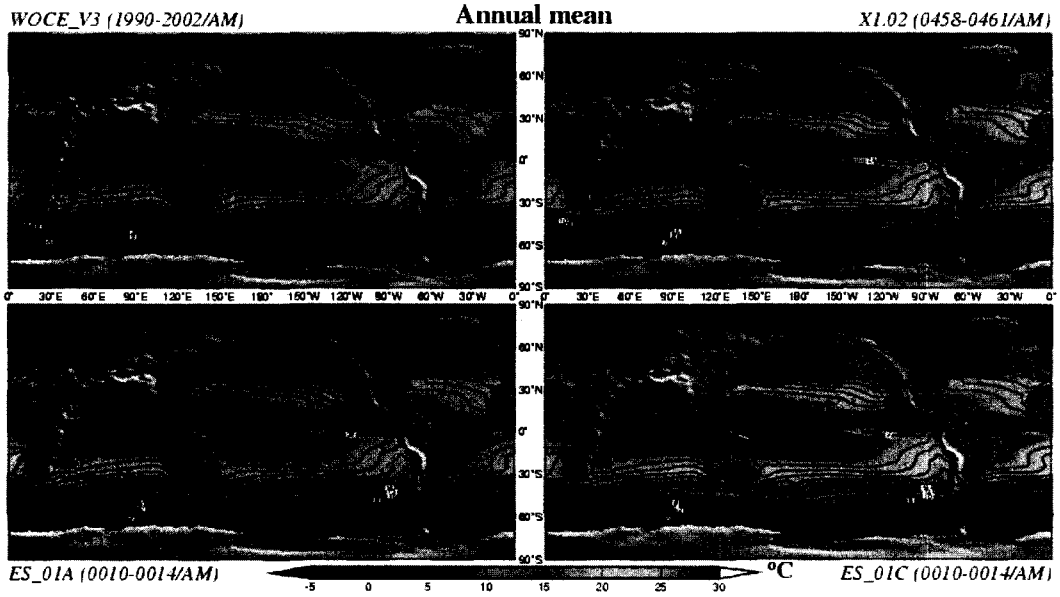

Fig. 1. Annual mean Sea Surface Temperature. WOCE V3 observation data (left top) and 0.1°×0.1° cases, baseline case (left bottom) and 1/3 times case (right bottom), are regrided by 1°×1° to compare with 1°×1° case (right top).

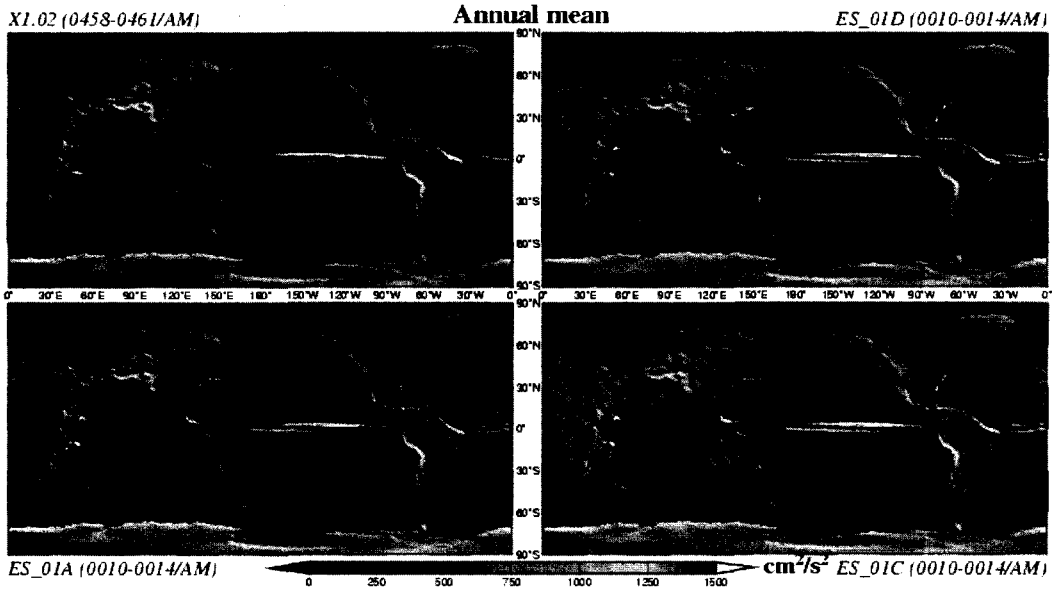

Fig. 2. Annual mean Horizontal Kinetic Energy, (U2+V2)/2. 1°×1° case (left top), 0.1°×0.1° case using GM scheme (right-top), 0.1°×0.1° baseline case (left-bottom), and 1/3 times 0.1°×0.1° case (right-bottom) are shown.

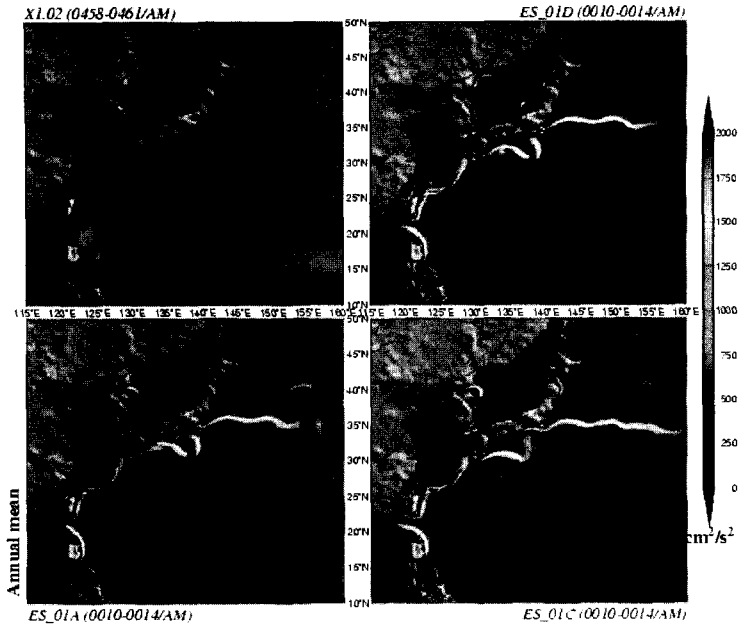

Fig. 3. Same as Fig. 2., except showing for Nowthwestern Pacific Ocean.

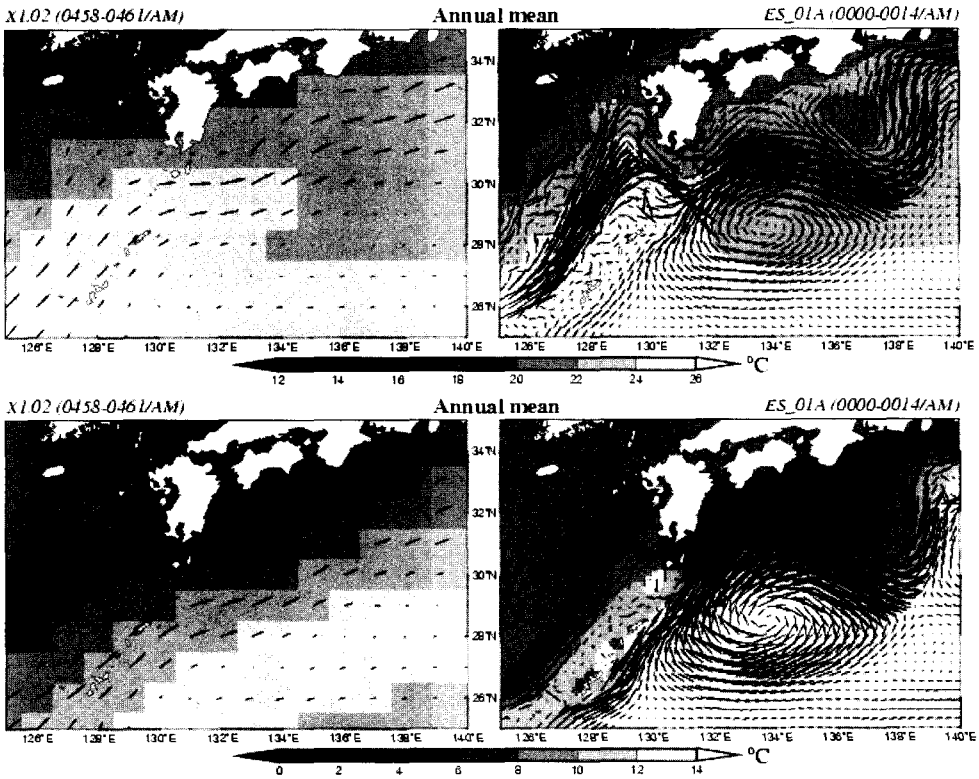

Fig. 4. Annual mean Currents and Potential Temperature. 1°×1° case and 0.1°×0.1° case are shown on left and right panel, respectively. Top panels show currents and temperature at surface level while bottom panels show those at 450 meter level.

The temperature structures (Fig. 5., middle panels) show the well-known ridge-trough system typical for most of the equatorial Pacific. The thermocline in 0.1°×0.1° resolution case (right middle panel) comes closest to the sea surface near 9°N at the northern flank of the countercurrent; a trough near 5°N indicates its southern flank. But those in 1°×1° resolution case (left middle panel) are shifted to north about 1°~2°. In the surface layer all cases reproduce well two cells of warmest water with temperatures above 28°C. However, 0.1°×0.1° resolution case is more accurate than 1°×1° resolution case.

The salinity distributions (Fig. 5., bottom panels) show water of lowest salinity associated with the north equatorial countercurrent. In the thermocline at depths between 100 and 150 m there are subsurface salinity maxima. They represent the cores of high salinity waters of subtropical origin. They are reproduced well in the southern hemisphere while it is located more northern part in the northern hemisphere.

The maximum mean geostrophic speed of the north equatorial countercurrent is well-positioned below the surface near 9°N between 50 and 100 m in the all cases. The equatorial undercurrent has a core speed of more than 90 cm/s but a deep westward flow at the equator below 250 m in observation data has not been seen in all simulation cases. The 0.1°×0.1° resolution case reproduces well the eastward-flowing deep countercurrents shown at 4°N and 4°S with a core near 250 m, while it is not easy distinguish that in the 1°×1° resolution case. The 0.1°×0.1° resolution case reproduce well the northern deep countercurrent connected with both the countercurrent and the undercurrent but the 1°×1° resolution case does not.

In general, the results from 0.1°×0.1° resolution case shows a more realistic profile that reproduces a distinctive thermocline and more uniform mixed layer, in agreement with observation data (Wyrtki and Kilonsky, 1984).

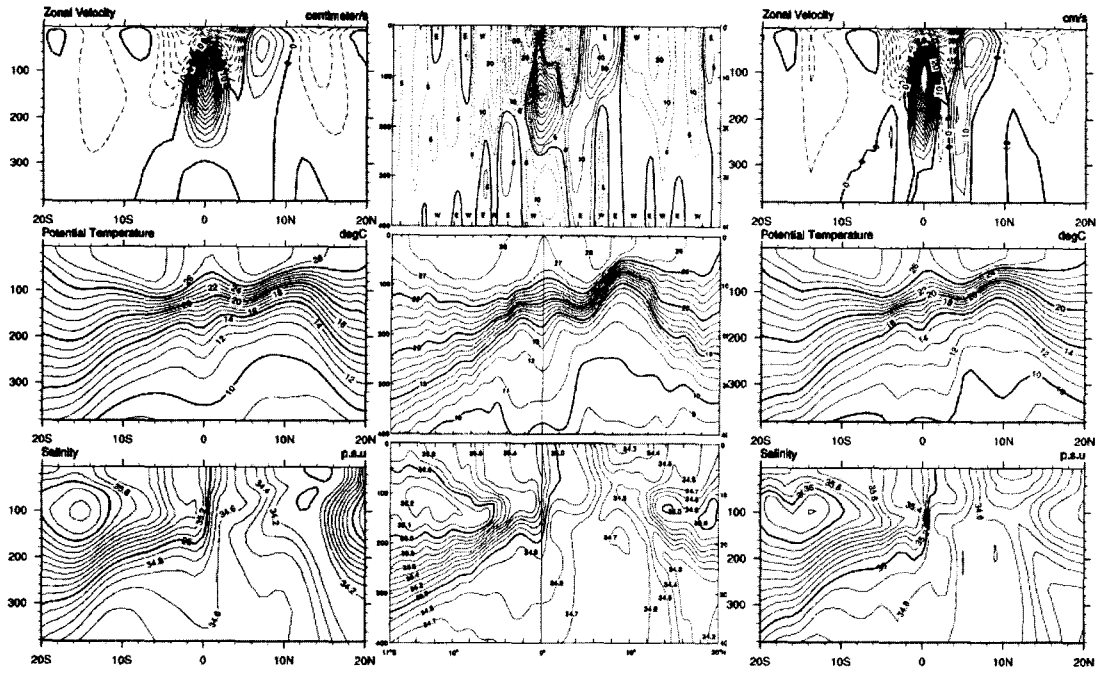

Fig. 5. (Center) Mean zonal geostrophic flow (cm/s), temperature (°C), and salinity (psu) between Hawaii and Tahiti and from 0~400 m, for the period April 1979 ~ March 1980. Adapted from Wyrtki and Kilonsky (1984). (Left) Annual mean fields calculated from the 1°×1° resolution model results along 155°W. (Right) Same as the left panel except 0.1°×0.1° resolution model.

4. CONCLUSION

This study examines the effect of horizontal grid resolution between eddy-permitting and eddy- resolving. We compare one simulation using a 1°×1° horizontal mesh to three simulations that use a 0.1°×0.1° horizontal mesh. Since 0.1°×0.1° resolution simulation can resolve mesoscale eddies, our results do assess the possible importance of resolving eddies. This paper has concentrated on a description of the time-mean circulation; thus our results do not assess possible sensitivity of simulated time variability to horizontal resolution.

While the eddy-resolving resolution does not lead to large changes in the mean flow patterns, the variability in the model is enhanced significantly, and in general, the results of 0.1°×0.1° resolution case are closer to observations than the results of 1°×1° resolution case are. In particular, the western boundary currents of the 0.1°×0.1° resolution simulations are more realistic. The eddy induced currents are important only in a few places in the ocean. The most significant eddy induced currents activity was found in western boundary currents, equatorial regions, and the Antarctic Circumpolar Current.

On the other hand, however, not all aspects of the circulation have improved with resolution. The East/Japan Sea is still represented very poorly. Particular attention is also directed toward the unrealistic stationary anticyclone in the east coast of Korea.

The results of Duffy et. al. (2002) suggests that other approaches to improving the solution of ocean-climate models will be more effective than increases in horizontal resolution outside the eddy-resolving regime.

Our results suggests that increases in horizontal resolution to inside the eddy-resolving regime will be more effective than other approaches such as improved numerical methods, better parameterizations of sub-grid-scale processes, or better forcing data.

In our study the solutions are strongly constrained by surface boundary conditions; a coupled ocean-atmosphere model might display stronger sensitivity to ocean model resolution.

ACKNOWLEDGMENTS

This study was performed under the Project for Sustainable Coexistence of Human, Nature and the Earth of the Ministry of Education, Culture, Sports, Science and Technology of the Japanese government. We used the Earth Simulator for the Project by courtesy of the Earth Simulator Center, JAMSTEC in Japan.

REFERENCES

Bryan, F. O., and Smith, R. D., 1998. Modeling the North Atlantic circulation: From eddy-resolving to eddy-permitting. *Int. WOCE Newsl.*, 33, 12-14.

Duffy, P. B., M. E. Wickett, and Caldeira, K., 2002. Effect of horizontal grid resolution on the near-equilibrium solution of a global ocean-sea ice model. *J. Geophys. Res.*, 107, 12-1~12-11.

McAvaney, B., et al., 2001. Model evaluation, in *IPCC Third Assessment Report*, Intergov. Panel on Clim. Change, Geneva.

McClean, J., Semtner, A. J., and Zlotnicki V., 1997. Comparisons of mesoscale variability in the Semtner-Chervin 1/4° model, the Los Alamos Parallel Ocean Program 1/6° model, and TOPEX/Poseidon data. *J. Geophys. Res.*, 102, 25203-25226.

Semtner, Jr, A. J., 1986. Finite-difference formulation of a world ocean model, in *Advanced Physical Oceanographic Numerical Modelling*, J. J. O'Brien, Ed., D. Reidel Publishing Company, Norwell, Mass., p. 187.

Smith, R. and Gent, P., Eds., 2002. Reference Manual for the Parallel Ocean Program (POP), Ocean Component of the Community Climate System Model (CCSM2.0). LAUR-02-2484.

Wyrtki, K., and Kilonsky, B., 1984. Mean Water and Current Structure during the Hawaii-to-Tahiti Shuttle Experiment. *J. Phys. Oceanogr.*, 14, 242-254.